

Application of Chemical and Thermal Analysis Methods for Studying Cellulose Ester Plastics

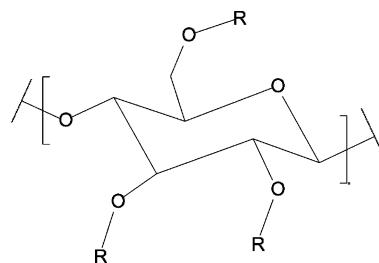
MICHAEL SCHILLING,* MICHEL BOUCHARD,
HERANT KHANJIAN, TOM LEARNER, ALAN PHENIX, AND
RACHEL RIVENC

The Getty Conservation Institute, Los Angeles, California

RECEIVED ON JANUARY 13, 2010

CONSPECTUS

Cellulose acetate, developed about 100 years ago as a versatile, semisynthetic plastic material, is used in a variety of applications and is perhaps best known as the basis of photographic film stock. Objects made wholly or partly from cellulose acetate are an important part of modern and contemporary cultural heritage, particularly in museum collections. Given the potential instability of the material, however, it is imperative to understand the aging mechanisms and deterioration pathways of cellulose ester plastics to mitigate decomposition and formulate guidelines for storage, exhibition, and conservation. One important aspect of this process is the ability to fully characterize the plastic, because variations in composition affect its aging properties and ultimate stability. In this Account, we assess the potential of a range of analytical techniques for plastics made from cellulose acetate, cellulose propionate, and cellulose butyrate.



Comprehensive characterization of cellulose ester plastics is best achieved by applying several complementary analytical techniques. Fourier-transform IR (FTIR) and Raman spectroscopy provide rapid means for basic characterization of plastic objects, which can be useful for quick, noninvasive screening of museum collections with portable instruments. Pyrolysis GC/MS is capable of differentiating the main types of cellulose ester polymers but also permits a richly detailed compositional analysis of additives. Thermal analysis techniques provide a wealth of compositional information and thermal behavior. Thermogravimetry (TG) allows for quantitative analysis of thermally stable volatile additives, and weight-difference curves offer a novel means for assessing oxidative stability. The mechanical response to temperature, such as the glass transition, can be measured with dynamic mechanical analysis (DMA), but results from other thermal analysis techniques such as TG, differential scanning calorimetry (DSC), and dynamic load thermomechanical analysis (DLTMA) are often required to more accurately interpret the results.

The analytical results from this study form the basis for in-depth studies of works of art fabricated from cellulose acetate. These objects, which are particularly at risk when stored in tightly sealed containers (as is often the case with photographic film), warrant particular attention for conservation given their susceptibility toward sudden onset of deterioration.

Introduction

Cellulose acetate (CA) was developed at the beginning of the 20th century primarily as a safe alternative to the highly flammable cellulose nitrate. A versatile material, it has been used in countless household objects such as textiles, tool handles, eyeglass frames, and children's dolls, but arguably its most significant application is as a base for photographic film.¹ Remarkable sculptures fashioned from cellulose acetate by Gabo, Moholy-

Nagy, and Pevsner captivate even after the plastic begins to show signs of deterioration.

Cellulose acetate falls into the category of semisynthetic polymers because it originates from cellulose, a renewable natural resource. The manufacturing process involves esterification of highly refined cellulose with acetic anhydride in the presence of sulfuric acid catalyst to form fully acetylated cellulose triacetate, followed by partial hydrolysis to remove acid catalyst and produce a

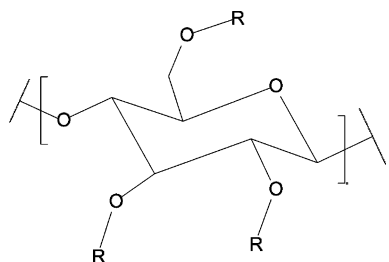


FIGURE 1. Structure of cellulose ester polymers.

degree of substitution in the polymer that yields the desired working properties.^{2,3} In most formulations, two or three hydrogen atoms on cellulose rings are substituted with acetate groups, creating di- and triacetate polymers (Figure 1). The properties of the final polymer can also be modified by introducing butanoic acid or propanoic acid to the reaction mixture, yielding cellulose acetate butyrate (CAB) or cellulose acetate propionate (CAP), respectively. CAP and CAB were introduced into the photographic film industry in 1924 and 1935, respectively.⁴ Working properties of cellulose ester polymers that are affected by these chemical modifications include hardness, impact resistance, moisture absorption, solubility, and weathering resistance.

Plasticizers are an important component of heat-molded cellulose ester plastics because the softening temperature lies close to the decomposition temperature.⁵ The most common plasticizers for cellulose ester plastics are diethyl phthalate, dimethyl phthalate, and triphenyl phosphate, but a wide variety of other plasticizers and additives have also been used (Figure 2).^{2,6}

Although several deterioration processes have a bearing on the stability of cellulose ester plastics in museum collections, hydrolysis of the ester side chain is, by far, the most significant.⁷ Hydrolytic loss of the acid side chain results in the liberation of organic acid, which causes further damage. In the case of cellulose acetate photographic film, collections are particularly at risk because they are commonly stored in tightly sealed enclosures that trap the acetic acid vapor. At some point, when the free acid content in the film reaches a critical level, the rate of free acid production exceeds the rate of diffusion, which causes the concentration of acetic acid to increase, and the hydrolysis reaction to become autocatalytic.⁶ Similarly, tightly sealed cases that house cellulose acetate objects can trap acetic acid vapor, posing risks to other objects in the case. Another deterioration mechanism is the alteration in plasticizer content through processes of migration or evaporation. ‘Doll’s disease’ causes the surface of children’s dolls made from cellulose acetate to become sticky with exuding plasticizer as the plastic ages. Plasticizers may also react with

chemicals in their surroundings to form other products, such as the reaction of triphenyl phosphate with water to form phenol and diphenyl phosphate, and the subsequent reaction of phenol with acetic acid form phenyl acetate and water.⁸ The final important degradation process is chain scission, whereby the polymer chain length is reduced, thereby weakening the material and leading to embrittlement. Ultimately, as a result of these deterioration processes, cellulose ester objects become prone to cracking, warping, discoloration, exudation, shrinkage, and powdering as they age.⁵

Objects made wholly or partly from cellulose acetate are an important part of modern and contemporary cultural heritage, particularly in museum collections. Due to the potential instability and dramatic deterioration of these objects, it is imperative to investigate aging mechanisms and deterioration pathways in order to be able to reduce the rates of deterioration and to formulate guidelines for their storage, exhibition, and conservation. One important aspect of this process is the ability to fully identify and characterize the plastic, because the variations in composition will affect the aging properties and ultimate stability.

In recognition of these significant needs, a consortium of mostly European institutions and laboratories involved in the care or study of modern and synthetic materials obtained funding from the European Commission to initiate a three-year project entitled Preservation of Plastic Artifacts in museum collections (POPART). The objective of the project is to develop a strategy to improve preservation and maintenance of three-dimensional plastic objects in museum collections, which includes cellulose acetate. Specific aims of the project include identifying risks associated with the exhibition, cleaning, protection, and storage of plastic artifacts, plus the establishment of recommended practices.⁹ The GCI is participating in the project as an unfunded partner.

In this Account, the potential for chemical analysis of plastics made from cellulose acetate, cellulose propionate, and cellulose butyrate using a range of analytical techniques was assessed. The techniques included pyrolysis–gas chromatography/mass spectrometry (Py-GC/MS), Fourier-transform infrared spectroscopy (FTIR), and Raman spectroscopy, which are widely used by conservation scientists for the chemical characterization of materials used in works of art. Several thermal analysis techniques were also used to measure a wide range of physical properties and chemical composition of cellulose ester plastics. Thermogravimetry (TG), differential thermal analysis (DTA), differential scanning calorimetry (DSC), thermomechanical analysis (TMA), and dynamic mechanical analysis (DMA) are important techniques that provide useful

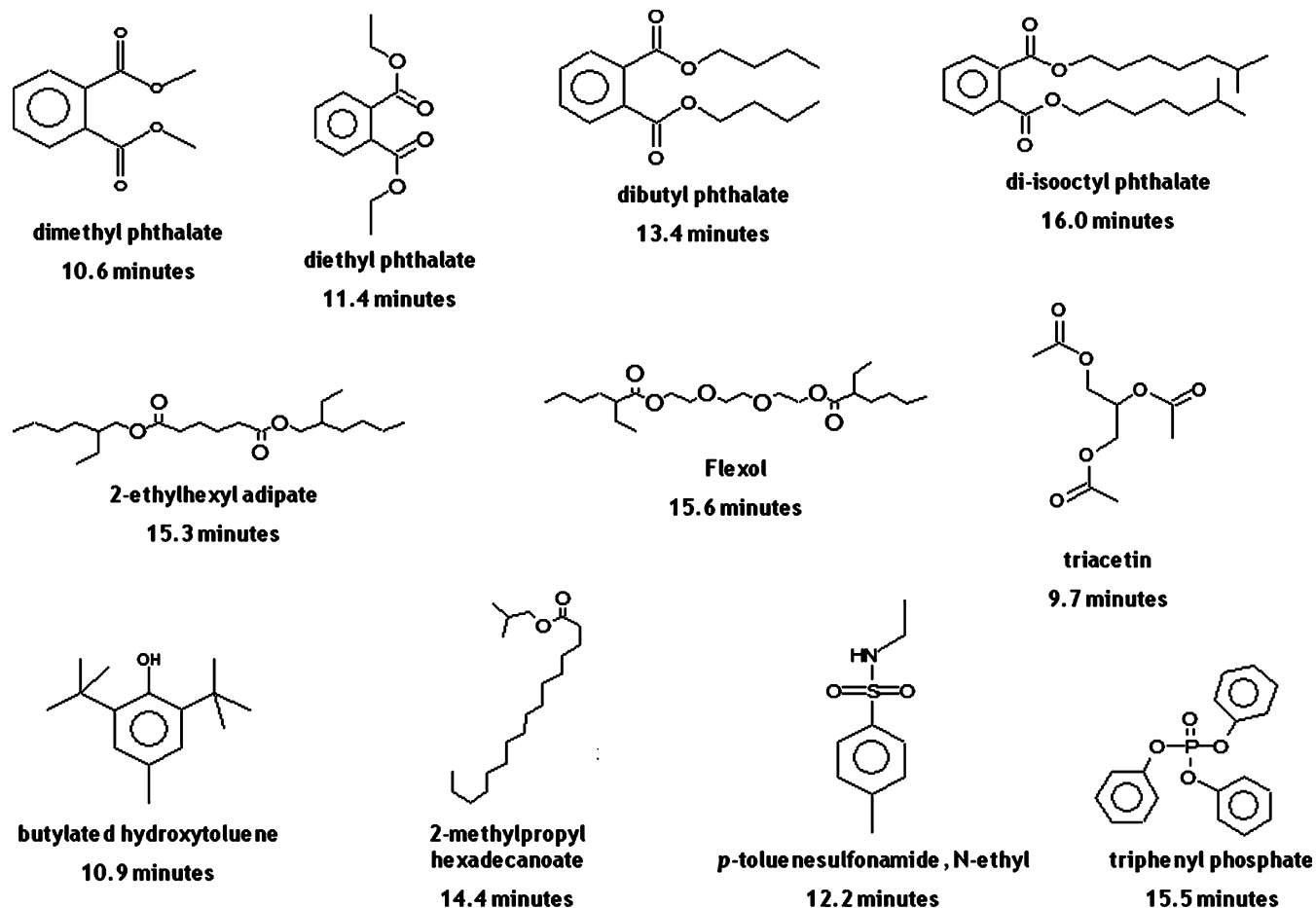


FIGURE 2. Additives used in cellulose ester plastics. Retention times obtained from the Py-GC/MS method are listed for the compounds.

information that complements chemical analysis data but are seldom applied to works of art because they require more sample material. These parameters include volatile content, thermal stability, oxidative stability, glass transition, melting point, storage and loss moduli, and $\tan \delta$. This Account also introduces the concept of “weight difference” curves, which permits a more accurate determination of polymer oxidation stability.

Samples

Samples of cellulose acetate (CA), cellulose acetate propionate (CAP), and cellulose acetate butyrate (CAB) were obtained from several sources. The ResinKit is a collection of 50 numbered specimens of various plastics from a distributor in Woonsocket, RI. Two ResinKits were available for testing: one set that was purchased in 2008 (abbreviated as NRK) plus an older collection purchased in 1984 (abbreviated as ORK). During the course of this research, it was discovered that some ResinKit samples are mislabeled; results in this study for ResinKit samples have been assigned the correct designation. In addition, POPART distributed to the

project partners a collection of 91 plastic reference samples, commercial items, and artifacts, which is called *SamCo*. Chemically pure powdered standards of CA, CAB, and CAP were purchased from Scientific Polymer Products, Inc. (no added plasticizers; abbreviated as SPP). Finally, a flexible sheet of CA was purchased from Goodfellow Cambridge Ltd. (abbreviated as GF).

List of Samples. Cellulose Acetate: SPP, GF, ORK11, SamCo #55A (transparent gray screwdriver), SamCo #55B (yellow knitting needle). Cellulose Acetate Propionate: SPP, SamCo #06 (NRK11), SamCo #07 (NRK12), SamCo #08 (NRK13). Cellulose Acetate Butyrate: SPP, SamCo #56 (orange screwdriver handle), SamCo #57 (XCelite screwdriver handle).

Experimental Procedures

FTIR. Small fragments of polymer were placed on a diamond window and flattened using a metal roller. Samples were analyzed using a 15 \times magnification Schwarzschild objective on a Bruker Optics, Inc., Hyperion 3000 FT-IR microscope with a

liquid nitrogen-cooled midband MCT detector, purged with dry air. The spectra were the sum of 64 scans at 4 cm^{-1} resolution.

Raman. Raman spectra were collected using a Renishaw InVia Raman microspectrometer coupled to a Leica DMLM microscope. After wavenumber calibration using the silicon peak at $520.5 \pm 1\text{ cm}^{-1}$, the samples were placed under the microscope objective ($L50\times/0.5$) for analysis. The laser used is a 785 nm diode HPNIR and the power was kept low to avoid degradation by laser heating ($\sim 50\text{ mW}$ on the sample). The acquisition time was 60–100 s from 100 to 4000 cm^{-1} with a 1200 L/mm grating and a Peltier-cooled CCD array detector. The spectral resolution was $\pm 2\text{ cm}^{-1}$.

Py-GC/MS. An Agilent 5975C inert MSD/7890A gas chromatograph/mass spectrometer and Frontier PY-2020D double-shot pyrolyzer were used. GC conditions: Ultra ALLOY-5 column ($30\text{ M} \times 0.25\text{ mm} \times 0.25\text{ }\mu\text{m}$), helium at 1 mL/minute , split injector at $320\text{ }^\circ\text{C}$ with 50:1 split ratio, no solvent delay. Oven program: 2 min at $40\text{ }^\circ\text{C}$, $20\text{ }^\circ\text{C/minute}$ to $320\text{ }^\circ\text{C}$, 9 min isothermal. MS conditions: 33–600 amu scanned at 2.59 scans/s, MS transfer line $320\text{ }^\circ\text{C}$, source $230\text{ }^\circ\text{C}$, MS quad $150\text{ }^\circ\text{C}$. Samples were placed into $50\text{ }\mu\text{L}$ stainless steel Eco-cups fitted with an Eco-stick. Some samples were treated with $3\text{ }\mu\text{L}$ of 25% tetramethyl ammonium hydroxide (TMAH) in methanol, which was added to the cup. After 3 min, the cup was placed into the pyrolyzer and purged with helium for 3 min, then pyrolyzed for 6 s at $550\text{ }^\circ\text{C}$. The pyrolysis interface was maintained at $320\text{ }^\circ\text{C}$.

TG/SDTA. A Mettler Toledo TGA/SD TA851e with STARE software, v. 8.10, was employed that permitted simultaneous TG and DTA measurements. After 3 min at $30\text{ }^\circ\text{C}$ to purge the furnace, samples were heated in open $70\text{ }\mu\text{L}$ alumina crucibles at $20\text{ }^\circ\text{C/min}$ to $1000\text{ }^\circ\text{C}$. The purge gas was either nitrogen or oxygen at 50 mL/min .

DSC. Samples were analyzed on a Mettler Toledo DSC822e instrument in open $40\text{ }\mu\text{L}$ aluminum pans from 20 to $180\text{ }^\circ\text{C}$ at a rate of $2\text{ }^\circ\text{C/min}$, using nitrogen purge gas at 50 mL/min .

DLTMA. A Mettler Toledo TMA/SDTA841e instrument was used for the analyses. Small blocks of sample approximately 0.5 mm on a side were placed between two fused silica disks on the sample platform. A dynamic probe force between 0.10 and 0.50 N was applied as a 0.08 Hz square wave. Samples were heated from 20 to $180\text{ }^\circ\text{C}$ at a rate of $2\text{ }^\circ\text{C/min}$ with nitrogen purge gas at 30 mL/min .

DMA. A Triton Technology DMA 2000 instrument was used in single cantilever bending mode (1 Hz frequency, $50\text{ }\mu\text{m}$ displacement) with free sample lengths of 2 mm . Sam-

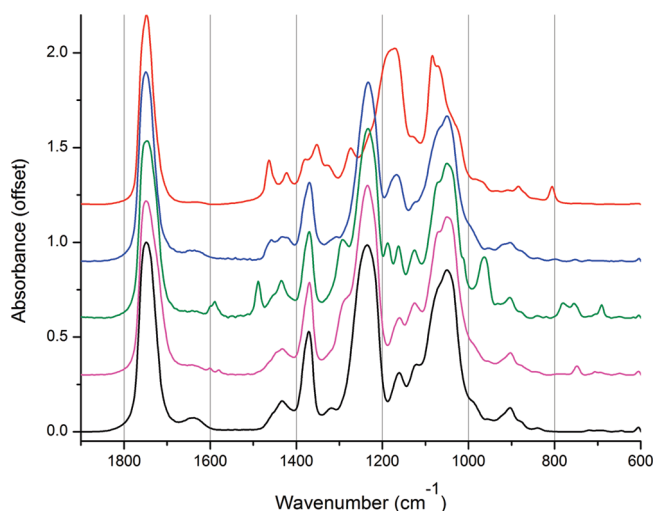


FIGURE 3. FTIR spectra ($1900\text{--}600\text{ cm}^{-1}$) for cellulose ester plastics. From top to bottom, CAP (SPP), CAB (SPP), CA (SamCo #55B), CA (SamCo #55A), CA (SPP).

ples were conditioned to the prevailing room environment (approximately 50% RH, $24\text{ }^\circ\text{C}$) prior to testing, but relative humidity was not controlled during testing. Samples were heated from ambient temperature to $180\text{ }^\circ\text{C}$ at a rate of $2\text{ }^\circ\text{C/min}$ in air.

Results

Preliminary characterization of cellulose ester objects and their major additives can be accomplished by FTIR and Raman spectrometry; portable versions of these instruments permit rapid, noninvasive analysis of entire collections of plastic objects.

The infrared spectra of the cellulose ester compounds (Figure 3) show three strong patterns of bands found in saturated molecules, typically referred to as “rule of three”. The first band at 1746 cm^{-1} is due to carbonyl stretch of the ester group, while the second band at 1234 cm^{-1} is due to asymmetric stretching of C–C–O of the ester group. The last large band appearing at 1049 cm^{-1} is the result of asymmetric O–C–C bond stretching attached to the carbonyl carbon. In addition, smaller bands located at 1370 and 1273 cm^{-1} are caused by methyl groups found in acetate and propionate esters, respectively. Other smaller bands present at 1589 , 1489 , and 960 cm^{-1} indicate the presence of additives such as triphenyl phosphate and phthalates.

A comparison of the Raman spectra of pure standards of CA, CAP, and CAB (Figure 4) showed that the differences among them are minor. However, few bands were reported to be specific for each of the different polymers.^{10–13} CAP, for example, has a very intense band at 1088 cm^{-1} that is much less intense in CAB and absent from the CA spectra. In the

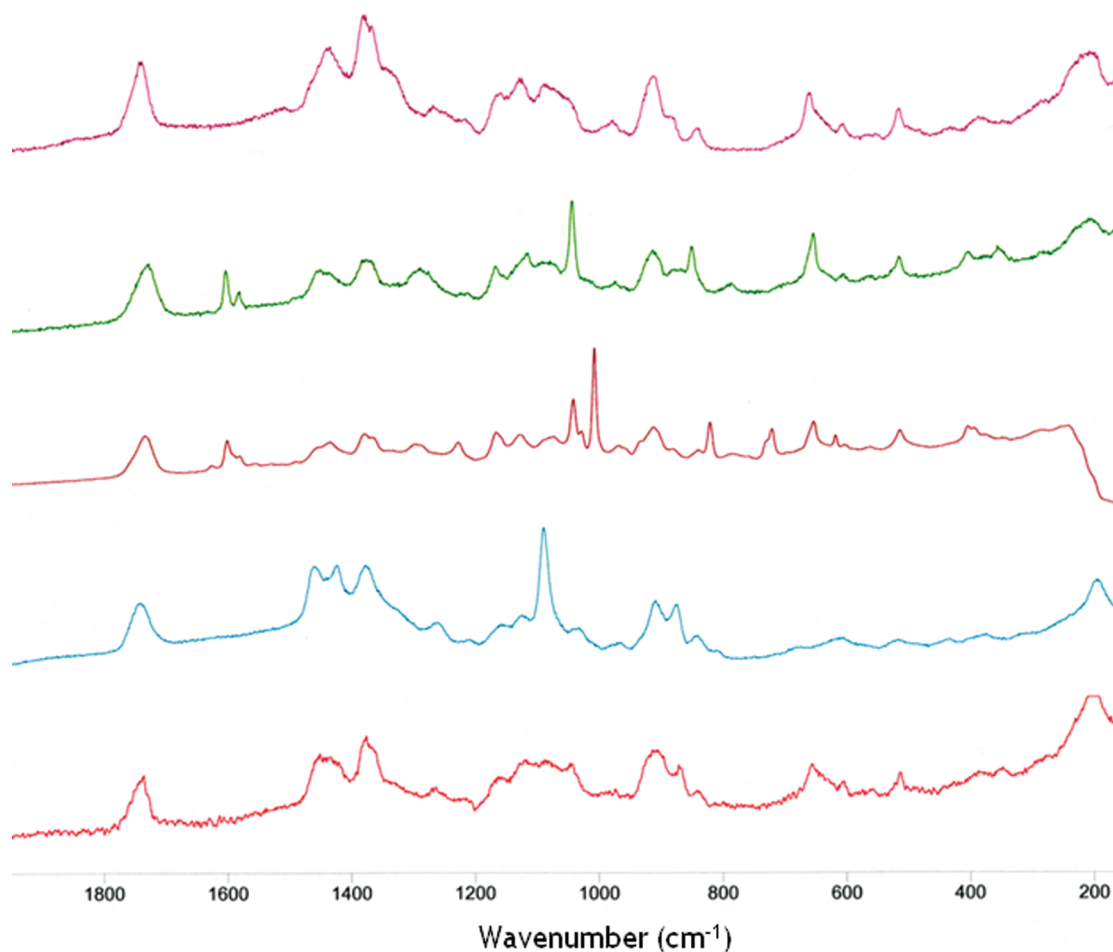


FIGURE 4. Raman spectra (200–2000 cm^{-1} region) for cellulose ester plastics. From top to bottom, CA (SPP), CA (GF), CA (SamCo #55B), CAP (SPP), CAB (SPP).

methyl stretching vibrations region (3000–2900 cm^{-1}), a strong band located at 2886 cm^{-1} in the spectra of CAP is absent in the CA spectra and shifted toward lower wavenumbers in the CAB spectra (2875 cm^{-1}). Finally, the single band at 1437 cm^{-1} in CA is observed as a strong and characteristic doublet in CAP at 1460 and 1423 cm^{-1} .

Evidence for plasticizers was also detected in the reference polymers. For example, four CA samples (GF, ORK11, SamCo #55A, and #55B) and CAB (ORK12) showed bands at 2875, 1724, 1600, 1578, and 1041 cm^{-1} , which are indicative of phthalates. Another plasticizer, triphenyl phosphate, was detected in CA (SamCo #55B) based upon characteristic Raman bands at 3075, 1006, and 726 cm^{-1} .

Py-GC/MS is capable of providing detailed compositional information of cellulose ester plastics and also detecting a wide range of additives even at very low concentrations, as well as in the presence of water.¹⁴ As Figure 5 shows, Py-GC/MS can easily differentiate CA, CAB, and CAP based upon the detection of short-chain organic acids that originate

from pyrolytic decomposition of the polymer side chains. Peaks for the acids appear fronted and poorly resolved in underivatized samples, whereas peaks for plasticizers and other additives are well-resolved and often dominate the resulting chromatograms because these compounds evaporate readily and do not decompose at pyrolysis temperatures. Small amounts of many additives were detected in the sample set in addition to large amounts of diethyl and dimethyl phthalate, adipate esters, and triphenyl phosphate. Additives are selected by their ability to impart specific desirable properties to the plastic depending on the end usage. For example, *N*-ethyl-*p*-toluenesulfonamide imparts flexibility, reduces water vapor permeability, and imparts resistance to oils, greases, and solvents,¹⁵ whereas TPP is a common flame retardant for CA.¹⁶ The fact that both of these additives were detected in SamCo #55B, a knitting needle, is consistent with these being desirable properties for a domestic product that is handled frequently.

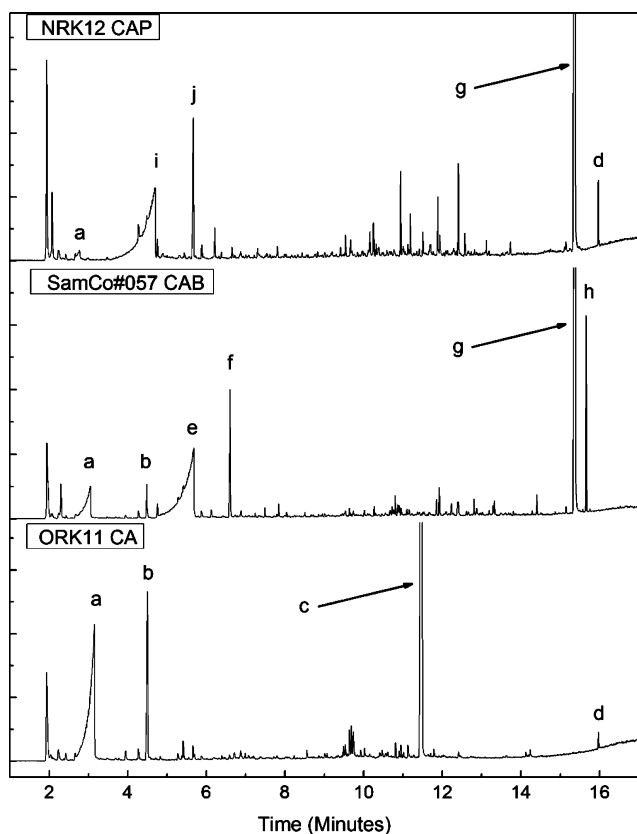


FIGURE 5. Py-GC/MS for CAP, CAB, and CA: (a) acetic acid; (b) 1,2-ethanediol monoacetate; (c) diethyl phthalate; (d) di-isoocetyl phthalate; (e) butanoic acid; (f) 2-hydroxyethyl butyrate; (g) 2-ethylhexyl adipate; (h) Flexol 3GO; (i) propanoic acid; (j) 2-hydroxyethyl propionate.

The main pyrolysis product of cellulose acetate is acetic acid from the acetate side chains.¹⁷ Improved detection of the acid side chains of the polymer may be achieved by converting them to methyl esters through the addition of TMAH prior to pyrolysis, as shown in Figure 6 for SamCo #55B. This reagent greatly improves the detection limits because methyl esters do not suffer from peak tailing to the same extent that the free acids do. Ideally, using this reagent, it might be possible to estimate the ratio of acetate to propionate or butyrate in CAP and CAB polymers, respectively, by measuring the relative amounts of methyl acetate, methyl propionate and methyl butyrate formed from TMAH-treated samples. One disadvantage of TMAH treatment evident in Figure 6 is the conversion of plasticizers to their methyl derivatives, which complicates the chromatograms and makes it difficult to identify the original additives.

Thermal analysis methods are excellent tools for characterizing plastics, although sample preparation is a critical, often overlooked, consideration. The rates of evaporation, oxidation, and many other chemical reactions and physical processes that thermal analysis techniques measure may be

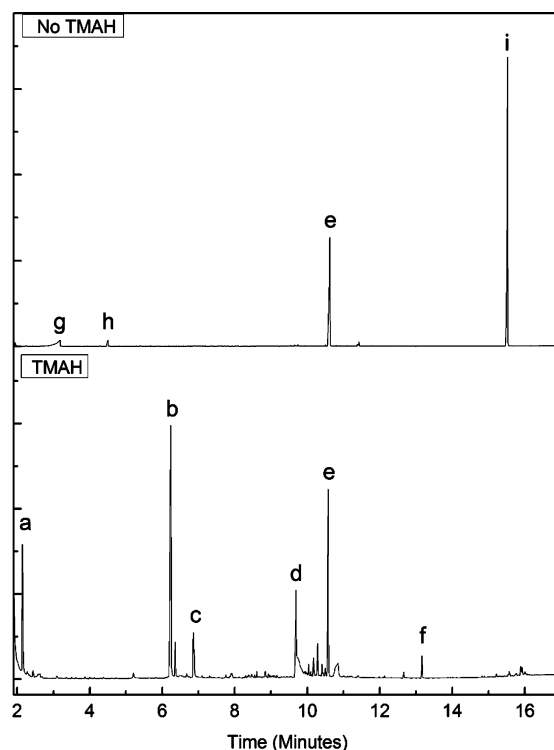


FIGURE 6. Effects of TMAH on Py-GC/MS results for CA (SamCo #55B): (a) methyl acetate; (b) trimethyl phosphate; (c) phenol; (d) phthalic acid; (e) dimethyl phthalate; (f) diphenyl methyl phosphate; (g) acetic acid; (h) 1,2-ethanediol monoacetate; (i) triphenyl phosphate.

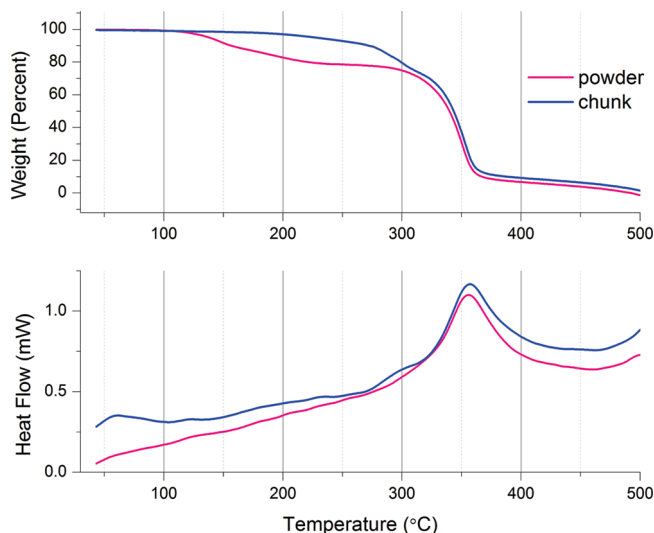


FIGURE 7. Effects of sample preparation on TG and SDTA results for Goodfellow CA.

affected by the homogeneity and surface to volume ratio of the sample. Accordingly, TG, DSC, and DTA often give optimum results for samples that have been powdered.

For example, Figure 7 shows the TG and DTA curves in oxygen for 1 mg of powdered CA that contains diethyl phthalate plasticizer with those for a 1 mg chunk of the same

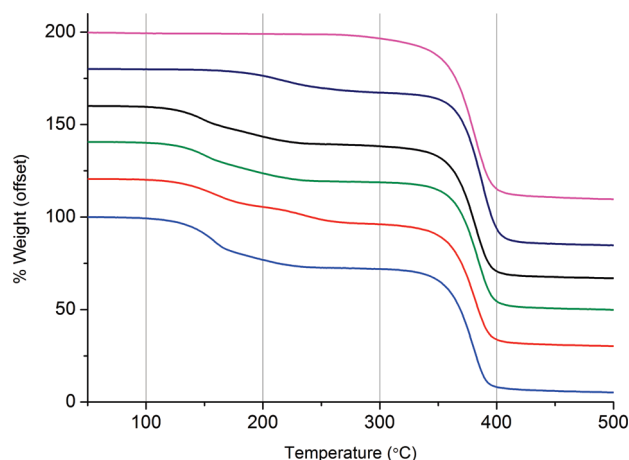


FIGURE 8. Evaporation of additives from cellulose ester plastics. From top to bottom, CA (SPP), CAP (NRK 11), CA (GF), CA (ORK 11), CA (SamCo #55B), and CA (SamCo #55A).

material. The powdered sample was produced using an abrasive tool, the Polymer Prepper, which is available from Frontier Laboratories. It is clear that evaporation of the plasticizer proceeds at a much lower temperature from the powdered material, whereas one might greatly underestimate the volatility of the plasticizer based on TG results for chunk samples. Considering that the surfaces of plastic CA objects often become more highly textured as they age, the rate of plasticizer loss could therefore increase over time, leading to further instability of the object. One other observation from the figure is that the onset of evaporation for plasticizers may be difficult to ascertain from the SDTA curves, especially for small samples, whereas the onset of oxidation is clearly evident because it is the main weight loss step.

While it is certainly possible to measure the concentration of additives in CA polymers using Py-GC/MS, developing suitable test protocols for the possible range of additives used in CA would be difficult. In comparison, TG affords a simple means of measuring the total content of volatile additives based on the magnitude of the initial weight loss step.^{18,19} As Figure 8 shows, no well-defined weight loss step is evident below 260 °C for the CA standard from SPP, whereas for the other CA samples the weight losses range from 20% to 30% (Table 1). In assessing the aging behavior of plasticized CA, TG can be an excellent tool for tracking changes in volatile plasticizer content.

Although hydrolysis is the predominant deterioration mechanism for most objects made from CA, photo-oxidation is also an important concern for CA objects on display.⁵ TG analysis in oxygen or air atmosphere is a traditional approach for measuring the oxidation stability of plastics. Traditionally, oxidation stability is defined as the temperature at the inter-

TABLE 1. Percent Weight Loss between 30 and 260 °C and Additives Identified by Py-GC/MS

| material | % weight loss | additives |
|-----------------|---------------|--|
| CA (SPP) | 0 | none |
| CA (GF) | 21 | diethyl phthalate |
| CA (ORK11) | 21 | diethyl phthalate |
| CA (SamCo #55B) | 21 | triphenyl phosphate, dimethyl phthalate, dibutyl phthalate, and <i>N</i> -ethyl- <i>p</i> -toluene sulfanamide |
| CA (SamCo #55A) | 28 | diethyl phthalate |

section of tangent lines drawn before and after the main oxidative TG weight loss step (Figure 9). This procedure works well for assessing the relative oxidation stability of a set of samples, but has the drawback of overestimating the absolute oxidation stability because many materials gradually lose volatiles prior to oxidation. To compensate for this limitation, a novel approach was developed²⁰ whereby volatile losses and thermal decomposition are measured by a TG analysis in nitrogen, and a second sample is tested in oxygen to assess the effects of oxidation. A weight difference curve is obtained by subtracting the nitrogen curve from the oxygen curve, as shown in Figure 9 for Goodfellow CA. The traditional onset of oxidation as measured from the oxygen curve is about 360 °C, whereas the initial deviation from zero in the difference curve occurs about 270 °C, implying that the plastic actually undergoes oxidation at a much lower temperature.

Visco-elastic behavior of cellulose ester plastics is routinely measured using dynamic-load thermomechanical analysis (DLTMA) and DMA, although complementary information obtained from TG and DSC may be helpful in interpreting the thermomechanical results. Figure 10 shows the DLTMA, DSC, and TG results for Goodfellow CA. The softening point is

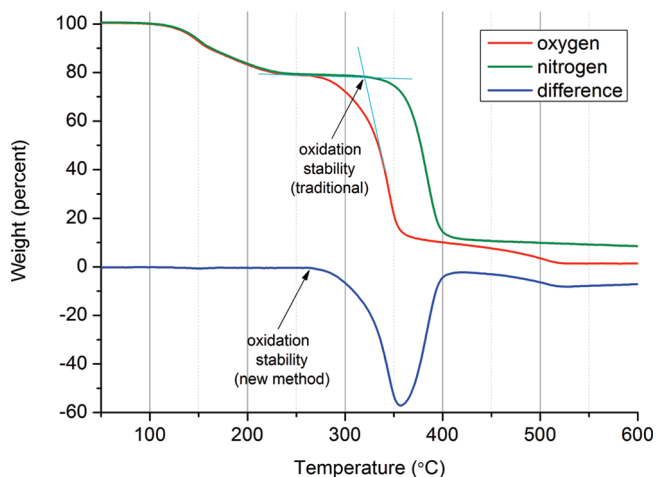


FIGURE 9. TG results for CA (ORK 11) in oxygen and nitrogen with weight difference curve. Evaluation of onset of oxidation indicated as intersection of tangent lines for oxygen curve (traditional method) and the deviation from the initial zero baseline in the weight difference curve (new method).

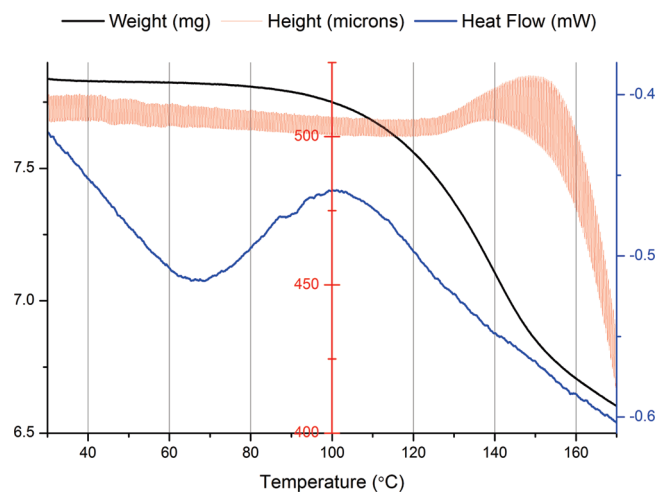


FIGURE 10. TG (black curve), DLTMA (red curve), and DSC (blue curve) results for Goodfellow CA.

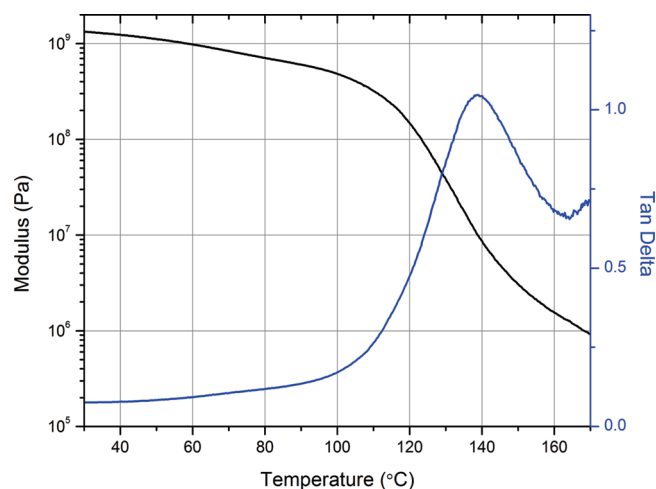


FIGURE 11. DMA Results for Goodfellow CA. Black curve is modulus; blue curve is $\tan \delta$.

TABLE 2. DMA Results for Cellulose Ester Plastics

| sample | mean temperature of 1 Hz $\tan \delta_{\max}$ (°C) |
|--------------------------------------|--|
| cellulose acetate (GF) | 138.9 |
| cellulose acetate propionate (NRK11) | 117.5 |
| cellulose acetate (ORK11) | 139.3 |
| cellulose acetate butyrate (NRK12) | 113.5 |

clearly evident in the DLTMA curve as the point at which the magnitude of the probe oscillations increases, which is approximately 130 °C. Comparing the DSC and TG results, there is little indication of the glass transition in the DSC curve, primarily due to the evaporation of plasticizer, which begins at approximately 80 °C. In contrast, the DMA results in Figure 11 show that the glass transition temperature lies at 139 °C, which corresponds to the maximum in the 1 Hz $\tan \delta$ curve (Table 2). Based on the results for the entire set of CA samples, it was observed that thermomechanical measurement, using either DMA or DLTMA, yielded a much clearer indica-

tion of the glass transition temperature than did DSC. One other factor known to affect the mechanical behavior of cellulose acetate is the equilibrium moisture content, because water can act as a coplasticizer.⁶ Thus, in conducting comparative studies, it would be advisable to control the relative humidity conditions in the sample storage chamber as well as in the analytical protocols.

Finally, in the DSC results of Figure 10, the broad initial endotherm that has a minimum at 65 °C was attributed to the evaporation of acetic acid from the plastic. In the TG results, the weight loss step corresponding to this peak was roughly 0.2%. It was observed that this peak and the related weight loss step are much larger in older samples of cellulose acetate, presumably because these samples are hydrolyzed to a greater extent than the much newer sample from Goodfellow. Future research will investigate the use of DSC and TG to assess the aging behavior of cellulose acetate.

Conclusions

The selection of analytical techniques to study cellulose ester polymers is influenced by the level of information required as well as the availability of samples. FTIR and Raman, which are available also in portable, noninvasive instruments, are useful for differentiating the main types of cellulose ester, yet lack the sensitivity to detect plasticizers and other additives that may be present at lower concentrations. Py-GC/MS can provide detailed information about the composition of the base polymer and a range of additives from minute samples. Thermoanalytic techniques, which require far larger samples, shed light on the mechanical behavior of the polymer and its response to temperature. Regarding thermoanalytic data, it is clear that interpretation is facilitated by the availability of results from several thermal analysis techniques in combination. In conclusion, the present study of commercial materials formulated from cellulose acetate demonstrates that multiple analytical techniques are capable of providing a wealth of compositional information, and establishes their value for studying works of art made from this highly versatile plastic.

This work was carried out within the framework of a project supported by the European Commission (FP7-ENV-2007): POPART, Agreement No. 212218.

BIOGRAPHICAL INFORMATION

Michael Schilling is a Senior Scientist in organic materials analysis at the Getty Conservation Institute (GCI), where he has worked since 1983. His research interests include furniture lac-

quers, natural and synthetic paint binding media, and color measurement. He has participated in GCI field projects to conserve wall paintings in China and Egypt and has taught numerous workshops in quantitative GC/MS analysis of binding media.

Michel Bouchard earned his Ph.D. in spectrometry and archaeometry from the National Natural History Museum of Paris. He joined the GCI in 2006 and works in the Collection Research Laboratory, where he characterizes materials on works of art using Raman microscopy, X-ray diffractometry, and other techniques.

Herant Khanjian, Assistant Scientist at the GCI, received a B.S. in chemistry from the California State University, Northridge, in 1988. In his 21 years at the GCI, his research interests have included use of FTIR to characterize paint media, plastics, photographs, and furniture lacquers.

Tom Learner is a Senior Scientist and head of Modern and Contemporary Art Research at the GCI, where he oversees scientific research projects in modern paints, outdoor painted surfaces, and preservation of plastics. Before joining the Getty in 2007, he was Senior Conservation Scientist at the Tate Gallery in London, where he coordinated a major collaborative research project into the conservation issues of modern paints. He holds a Ph.D. in Chemistry from the University of London and a Diploma in Conservation of Easel Paintings from the Courtauld Institute of Art.

Alan Phenix holds the position of Scientist at the GCI. Prior to joining the GCI in 2006, he was a practitioner and educator in paintings conservation in universities in the United Kingdom and Norway for over 15 years. He is presently editor in chief of *Studies in Conservation*.

Rachel Rivenc graduated from Paris I Sorbonne in paintings conservation in 2001. She has been a member of the Modern and Contemporary Art Research group since 2007. Presently, she is a Ph.D. candidate at Mnhm/CRCC, Paris, studying automotive and industrial paints used for contemporary outdoor sculptures.

REFERENCES

1 <http://azom.com>. Accessed July 2009.

- 2 Hon, D. N. S. Cellulose plastics. In *Handbook of Thermoplastics*; Olabisi, O., Ed.; Marcel Dekker: New York, 1997; pp 331–347.
- 3 Lewin, M. *Handbook of Fiber Chemistry*, 3rd ed.; CRC Press, Boca Raton, FL, 2007; p 779.
- 4 <http://videopreservation.stanford.edu/library>. Accessed July 2009. An excellent summary of the problems related to film storage is provided by history_science storage of acetate base film 16b.pdf.
- 5 Ballany, J. Littlejohn, D. Pethrick, R. A. Quye, A. Probing the factors that control degradation in museum collections of cellulose acetate artefacts. In *Historic Textiles, Papers, and Polymers in Museums*; Cardamone, J. M., Baker, M. T. American Chemical Society: Washington, DC, 2001; pp 145–165.
- 6 Wypych, G. *Handbook of Plasticizers*; William Andrew Inc: New York, 2004; pp 278–282.
- 7 Tsang, J.; Madden, O.; Coughlin, M.; Maiorana, A.; Watson, J.; Little, N. C.; Speakman, R. J. Degradation of 'Lumarith' Cellulose Acetate: Examination and Chemical Analysis of a Salesman's Sample Kit. *Stud. Conserv.* **2009**, *54* (2), 90–105.
- 8 Louvet, A. Gillet, M. Les clichés photographiques sur supports souples: contribution à l'étude de leur stabilité, in *Les Documents Graphiques et Photographiques: Analyse et Conservation*; Archives de France: Paris, 1999; pp. 109–157.
- 9 <http://popart.mnhn.fr/>.
- 10 Schrader, B. *Raman/Infrared Atlas of Organic Compounds*, 2nd ed.; VCH: New York, 1989.
- 11 Kuptsov, A. H. Zhizhin, G. N. *Handbook of Fourier Transform Raman and Infrared Spectra of Polymers*; Elsevier: New York, 1998.
- 12 Firsov, S. P.; Zbankov, R. G. Raman Spectra and Physical Structure of Cellulose Triacetate. *J. Appl. Spectrosc.* **1982**, *37* (2), 940–947.
- 13 Lin-Vien, D. Colthup, N. B. Fateley, W. G. Grasselli, J. G. *Handbook of Infrared and Raman Characteristic Frequencies of Organic Molecules*; Academic Press: Boston, MA, 1991.
- 14 Learner, T. J. S. *Analysis of Modern Paints*; J. Paul Getty Trust: Los Angeles, CA, 2004; pp 38–80.
- 15 Bergen, H. S., Jr.; Craver, J. K. Sulfonamide Plasticizers and Resins. *Ind. Engin. Chem.* **1947**, *39* (9), 1082–1087.
- 16 Ormsby, M. Analysis of Laminated Documents Using Solid-Phase Microextraction. *J. Am. Inst. Conserv.* **2005**, *44* (1), 13–26.
- 17 Moldoveanu, S. *Analytical Pyrolysis of Natural Organic Polymers*; Elsevier Science B.V.: Amsterdam, 1998; p 258.
- 18 Gillmor, J.; Seyler, R. J. Using chemistry in compositional analysis by thermogravimetry. In *Compositional Analysis by Thermogravimetry, STP 997*; Earnest, C. M., Ed.; ASTM: Philadelphia, PA, 1988; pp 38–47.
- 19 Wendlandt, W. W. *Thermal Methods of Analysis*, 2nd ed.; Elving, P. J., Kolthoff, I. M., Eds.; Chemical Analysis, Vol. 19; John Wiley and Sons: New York, 1974; pp 123–125.
- 20 Schilling, M. R. M.Sc. Thesis, California State Polytechnic University, Pomona, CA, 1990, pp 62–94.